COMPLEX APPROACH TO REMOTE THERMAL SENSING OF THE ATMOSPHERE

B.P. Ivanenko and K.I. Gobrusenko

Institute of Atmospheric Optics,
Siberian Branch of the Russian Academy of Sciences, Tomsk
Received January 8, 1992

A complex approach to solving the problem of remote thermal sensing of the atmosphere is proposed. It is based on joint processing of data of active (lidar) and passive (radiometer) satellite remote sensing of the atmosphere. Some methods are considered for solving the inverse problems of spaceborne IR radiometry which allow one to assimilate and employ the information about the reconstructed temperature profile obtained from spaceborne lidars. The efficiency of algorithms are investigated in numerical experiments.

In recent years active lidar sounding techniques have attracted an increasing attention in addition to conventional passive methods of remote thermal sounding of the atmosphere (RTSA). Thus within the framework of the program "Schuttle Atmospheric Lidar System" a numerical simulation of double– and three–frequency lidar systems was carried out. It was intended for the RTSA based on the method of separating out aerosol and molecular components in the received lidar returns.[1,2] It turned out that the advantage of the lidar method is its higher vertical resolution (0.2–2 km) as compared to passive methods of the RTSA and its disadvantage is a limited lifetime of lidar operation, substantial energy consumption, low horizontal resolution (200–3000 km), and possible bias of the reconstructed temperature profile due to the errors in *a priori* assignment of the spectral behavior of the aerosol and molecular light scattering coefficients when the aerosol and molecular components are separated out in the received lidar returns.

Described in this paper is a complex approach to solution of the RTSA problem which is based on the joint processing of the data of active (lidar) and passive (radiometer HIRS–II) satellite–based RTSA. In so doing the spaceborne lidar is used for qualitative reconstruction of temperature profile at high spatial resolution with subsequent incorporation of them into a mathematical scheme for processing of data obtained from the HIRS–II. This, in turn, requires a creation of specialized algorithms for solving the inverse problems (IP) of the RTSA which could allow one to assimilate and employ the information about the reconstructed temperature profiles obtained from spaceborne and ground–based lidars as well as data of radiosonde observations and contact measurements.

1. ALGORITHMS FOR SOLVING IP OF THE COMPLEX RTSA

As is well known, the passive method of the RTSA is based on solution of an integral radiation transfer equation whose simplest linearized analog can be written in the form[2]

$$I(\nu) = B[\nu, T(1)]P[\nu, T(1)] - \int_0^1 K(\nu; B[\nu; T(\xi)]) B[\overline{\nu}; T(\xi)] \, d\xi, \quad (1)$$

where $I(\nu)$ is the intensity of outgoing radiation with the contribution of the underlying surface at the frequency ν,

taken into account $B[\overline{\nu}, T(\xi)]$ is the linearized Planck function at some central frequency $\overline{\nu}$, $P[\nu, T(\xi)]$ is the function of atmospheric transmission, $K(\nu, B[\nu, T(\xi)]) = dP[\nu, T(\xi)]/d\xi$ is the kernel of Eq. (1), $T(\xi)$ is the temperature profile, P is the pressure, $\xi = p/p_0$ is the variable of integration, and p_0 is the pressure near the Earth's surface.

Different physical and mathematical aspects of solution of Eq. (1) as applied to the RTSA are described in detail in Refs. 2 and 3.

In what follows using a particular example, we examine the scheme for constructing a specialized algorithm for processing of data of a complex RTSA and in the numerical experiment we study its efficiency and accuracy characteristics.

For brevity and simplicity, we write down Eq. (1) in the operator form

$$K \mathbf{b} = \mathbf{I} , \quad (2)$$

where $\mathbf{b}$ is the solution vector of dimensionality n, $\mathbf{I}$ is the vector of the right–hand side of the dimensionality m, and K is the matrix operator of the dimensionality $m{\times}n$ corresponding to the kernel of Eq. (1). It is possible to construct such an operator to the best advantage (or to make algebraization of Eq. (1)) only by analyzing physical properties of the problem under study. First, it is necessary to take into account the fact that the vector $\mathbf{I}$ has small dimensionality (the number of recording channels does not exceed 7–10). On this basis, in contrast to Refs. 2 and 3, for algebraization of Eq. (1) the method, which has been proposed in Ref. 4, was used for solving the inverse problem of laser multifrequency sounding of the atmosphere. The essence of this method is as follows.

We choose the system of nodes $\{\xi_l\}$, $l = 1, 2, \dots, n$ in the region of the function $b(\xi)$ definition and assume that the function $b(\xi)$ is described analytically for each internal interval $[\xi_l, \xi_{l+1}]$. In this case it should be noted that this assumption does not hold for the peculiarities of behavior of the kernel of Eq. (1) for all $[\xi_l, \xi_{l+1}]$.

For the sake of simplicity let us assume, in contrast to Ref. 4, that the function $b(\xi)$ is approximated not with a quadratic parabola, but with a straight line, i.e., $b(\xi) = a_l + d_{l+1}\xi$ for all $[\xi_l, \xi_{l+1}]$.

The coefficients a_l and d_l, in turn, are determined in terms of the value $b(\xi_l)$. Moreover, according to Ref. 4, one can readily obtain the expression for replacing Eq. (1) by the corresponding sum

$$\int_0^1 K(v;\xi)\, b(\xi)\, \mathrm{d}\xi = \sum_{l=1}^{n-1}\int_{\xi_l}^{\xi_{l+1}} K(v_i;\xi)\,[a_l + d_{l+1}\xi]\,\mathrm{d}\xi = \sum_{i=1}^{n-1} Q_{i,\,l}\, b_l,$$

(3)

$$i = 1, 2, \ldots, m,\ l = 1, 2, \ldots, n,$$

where $K(v;\xi) = K(v; B[v, T(\xi)])$, and the coefficients of quadratures $Q_{i,\,l}$ are determined using the values of the kernel of the equation and the grid nodes.[4] The integrals in Eq. (3) can be calculated with any precision since the kernel of the equation is defined at any point of the interval $[\xi_l, \xi_{l+1}]$. Note that with such an approach to algebraization of initial equation (1) it is possible to reduce the dimensionality of the matrix of the operator K by a factor of two to four (keeping at the same time the required accuracy of the quadrature formula (3)). This, in turn, results in an essential increase of the operation speed of the algorithm for solving the IP that is of particular importance in the systems of operative processing of the satellite–measurement results.

We are coming now to the problem of constructing the algorithm for solving the IP. In Refs. 3 and 4 the authors used the method of Tikhonov's smoothing functional (TSF) for solving the inverse problem of the RTSA. This function was constructed based on limitation on the degree of smoothness of unknown solution. In this case the TSF takes the form

$$T_\alpha[b] = \|\hat{K}b - I\|^2_{L_2} + \alpha\, \|b\|^2_{W_2^1},$$

(4)

where α is the regularization parameter.

However, in our case the TSF must be constructed reasoning from the presence of *a priori* information about the reconstructed profile $b(\xi)$. In the simplest case some simulated profiles $b_m(\xi) = B[v, T_m(\xi)]$, where $T_m(\xi)$ is the climatic average profile of temperature, can serve as the aforementioned information. In a complex RTSA the temperature profile obtained from lidar or radiosonde data can be used as the climatic average profile of temperature. The TSF can be constructed on the basis of limitation on the norm of a solution deviation from the model. In so doing, the TSF takes the form

$$T_\alpha[\Delta b] = \|\hat{K}(\Delta b) - \Delta I\|^2_{L_2} + \alpha\, \|\Delta b\|^2_{W_2^1},$$

(5)

where $\Delta b = b - b_m$ and $\Delta I = I - I_m = I - K\, b_m$.

It should be noted that such a method was used elsewhere by one of the authors of this paper for processing the results of laser sounding of the atmospheric ozone[5] as well as by the authors of Refs. 3 and 6 for solving the IP of the RTSA using the method of statistical regularization.

Consider now the problem on minimizing functionals (4) and (5). It is well known[7] that this problem can be solved either by direct minimization of functionals (4) and (5) or by reducing this problem to the Euler equation for the TSF. In this paper the method of conjugate gradients (MCG) was used for minimizing functionals (4) and (5). The advantages of this method are the guaranteed convergence, easy computer performance, and possible creation of different modifications depending

on the presence of one or another additional information about the reconstructed profile $T(\xi)$. This can be the information about the presence and height of temperature inversions, information about a possible value of deviation of $T(\xi)$ form $T(\xi)$. In the latter case the problem of minimizing functionals (4) and (5) can be solved under restrictions in the form of inequalities and so on.

To study the efficiency of the proposed method for solving the IP of the RTSA a series of numerical experiments has been conducted. The results of these experiments are discussed below.

2. A SCHEME OF NUMERICAL EXPERIMENT

In calculations it was assumed that the outgoing radiation was measured in the 15–μm CO_2 absorption band using an IR radiometer HIRS–II incorporated into the instrumentation TOVS of the NOOA satellite (the central frequencies were 669, 680, 690, 703, 716, and 733 cm^{-1}). For temperature models we used the model profiles T_{m1} (midlatitude summer) and T_{m2} (tropical model) on which the perturbations $\Delta T_{1,2}(\xi)$ were imposed. Thus $T_1(\xi) = T_{m1}(\xi) + \Delta T_1(\xi)$, $T_2(\xi) = T_{m2}(\xi) + \Delta T_2(\xi)$, and $\Delta T_1(\xi)$ and $\Delta T_2(\xi)$ were chosen based on the data from Ref. 3. The simulation was aimed at studying the accuracy characteristics and the comparative analysis of calculational schemes (4) and (5) and the method of statistical regularization. When the climatic average profiles were used as *a priori* model, $T_{1,2}(\xi)$ was reconstructed at 21 points. At the same time, using a random–number generator, relative error of the order of 1% was introduced into the left hand–side of Eq. (1), which was consistent with real errors in recording the outgoing radiation intensity $I(v)$ with a radiometer HIRS–II.

The regularization parameter was chosen using the method of generalized discrepancy with the subsequent correction based on the quasioptimal criterion.[7] The atmospheric transmission functions $P[n, T(\xi)]$ and the kernel of Eq. (1) were calculated using the approximation methods.[8] In studying the efficiency of the complex approach to the solution of the IP of the RTSA (spaceborne lidar + radiometer) the temperature profiles were reconstructed using scheme (5), but in this case the temperature profile obtained from the lidar data, $T_L(\xi)$, was used as an *a priori* profile $T_m(\xi)$. To this end, numerical simulation of the experiment on the RTSA was made for a spaceborne three–frequency lidar with the energy characteristics given in Ref. 1. However, in contrasts to Ref. 1, where the temperature profile $T_s(\xi)$ was reconstructed based on the method of separating out the aerosol and molecular components in lidar returns, we used the regularization algorithms for processing of the optical sounding data.

Reconstruction of the profile $T_s(\xi)$ was accomplished at 41 points with 1 km vertical and 100 km horizontal resolutions and was of qualitative character, i.e., only the altitude and the sign of deviation of real temperature profile $T_s(\xi)$ from the climatic average one were determined. The values of thus obtained $\Delta T_s(\xi)$ and $T_s(\xi)$ were included into the mathematical scheme of processing of data obtained with the radiometer HIRS–II.

The detailed description of this method for reconstructing the temperature profile and estimating of its efficiency are beyond the scope of this paper and will be given in the subsequent publications.

We now turn to the discussion of the results of numerical simulation.

3. RESULTS OF NUMERICAL SIMULATION

Depicted in Fig. 1 are the results of reconstructing the simulated temperature profile $T_s(\xi)$ obtained by the calculational scheme (4). For comparison Fig. 2 presents the same data obtained using scheme (5).
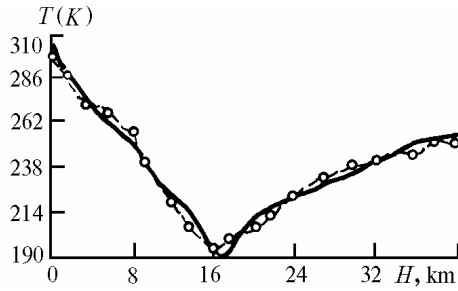
FIG. 1. Results of numerical experiment on reconstructing the simulated temperature profile: solid curve is the exact values $T_2(\xi) = T_{m2}(\xi) + \Delta T_2(\xi)$ and dotted curve is the values of $T_{2a}(\xi)$ reconstructed by scheme (4).
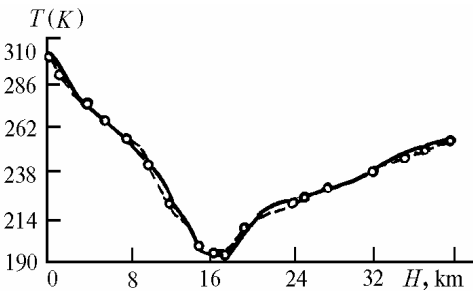
FIG. 2. Results of numerical experiment on reconstructing the simulated temperature profile: solid curve is the exact values $T_2(\xi) = T_{m2}(\xi) + \Delta T_2(\xi)$ and dotted curve is the values of $T_{2a}(\xi)$ reconstructed by scheme (5), with the a priori profile being the climatic average profile.
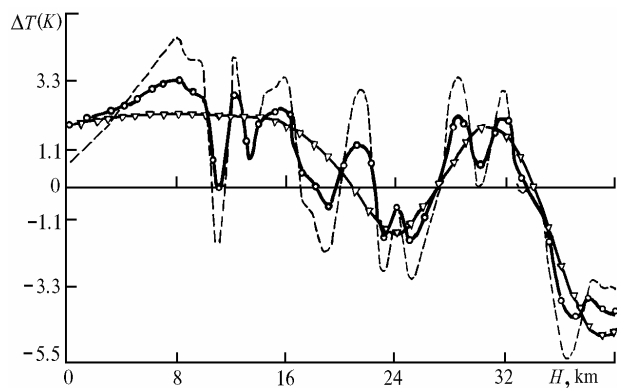
FIG. 3. Results of numerical experiment on the complex remote thermal sensing of the atmosphere: dashed curve is the exact values of $\Delta T_3(\xi)$, dotted curve is the values $\Delta T_{3a}(\xi)$ reconstructed by scheme (5), with the a priori profile being the lidar one, and curve with triangles presents the values of $\Delta T_{3a}(\xi)$ reconstructed by scheme (5), with the a priori profile being the climatic average one.

The climatic average profile of temperature $T_{m2}(\xi)$ was used as an *a priori* model.

Figure 3 presents a good illustration of the efficiency of the complex approach to solution of the IP of the RTSA when $\Delta T_s(\xi)$ is reconstructed by scheme (5) with the *a priori* model of the temperature profile reconstructed from lidar data.
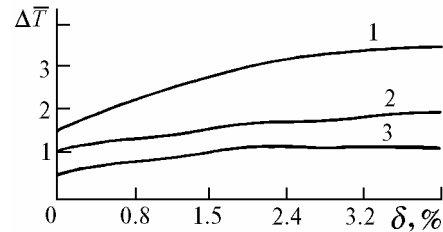
FIG. 4. Mean error of reconstructing temperature profiles $\Delta \overline{T}$ as a function of errors in recording the outgoing radiation intensity δ. 1) reconstructed by scheme (4) without a priori *information, 2) reconstructed by scheme (5),* a priori *profile is the climatic average one, and 3) reconstructed by scheme (5),* a priori *profile is the lidar one.*

TABLE I. Comparison of interpretation methods.

Method of reconstructing	$\dfrac{\Delta \overline{T}}{\Delta T_{max}}$	$T_1(\xi)$	$T_2(\xi)$
Scheme (4), TSF method	$\Delta \overline{T}$	2.2	3
	ΔT_{max}	4.0	4.2
Scheme (5), TSF method with *a priori* information	$\Delta \overline{T}$	1.2	1.1
	ΔT_{max}	2.3	2.2
Method of statistical regularization with adequate statistics	$\Delta \overline{T}$	1.8	1
	ΔT_{max}	3.8	2.3
Method of statistical regularization with inadequate statistics	$\Delta \overline{T}$	3.5	2.6
	ΔT_{max}	10	5.6

Figure 4 and Table I, by analogy with Ref. 3, give the results of estimating the accuracy characteristics of the $T_{1,2}(\xi)$ reconstruction depending on the scheme of the RTSA data interpretation. Here $\Delta \overline{T} = \sum\limits_{i=1}^{n} |T(\xi_i) - T_\alpha(\xi_i)|/n$ characterizes some mean deviation of the reconstructed profile $T_\alpha(\xi)$ from an actual one $T(\xi)$ and ΔT_{max} is the maximum deviation of $T_\alpha(\xi)$ from $T(\xi)$.

4. CONCLUSIONS AND RECOMMENDATIONS

We can infer from the simplest qualitative analysis of the graphic information presented in Figs. 1–3 that algorithm (5) possesses high efficiency compared to the standard scheme of the TSF. At the same time, by analyzing quantitative estimates of the accuracy characteristics of reconstructing temperature profiles $\Delta \overline{T}$ and ΔT_{max} listed in Table I it is possible to draw the following conclusions.

1. The method of statistical regularization, in the presence of adequate statistics, is preferable compared to the TSF method, since $\Delta \overline{T}$ determined by the method of statistical regularization equals 1–2 K, while $\Delta \overline{T}$ obtained by the TSF method is from 2 to 3 K.

2. If the statistics is inadequate the TSF method is proved to be more useful, since $\Delta\overline{T}$ calculated by the method of statistical regularization runs between 2.5 and 3.5 K, while ΔT_{max} can reach from 6 to 10 K.

The values $\Delta\overline{\overline{T}}$ obtained by scheme (5) and by the method of statistical regularization for adequate statistics, are practically of the same value. In its turn, the value ΔT_{max} obtained by scheme (5) is much smaller than that of ΔT_{max} obtained by the method of statistical regularization in the case of inadequate statistics.

It should also be noted that scheme (5) to be performed needs for much less *a priori* information than the method of statistical regularization does and it can readily be performed on a computer. One more advantage of calculational scheme (5), when it is used for processing of the data at stations of regional reception of information from satellites, is its ability to assimilate practically any *a priori* information about the temperature profile under reconstruction. These can be the results of radiosonde observations, lidar and sodar data, and the results of contact measurements obtained from aircrafts, ground–based meteorological stations and so on. In this case, the *a priori* data can be without statistical basis and, moreover, can be of a purely qualitative character, e.g., height and sign of thermal inversion obtained from the sodar, the lower boundary height and optical characteristics of cloudiness obtained based on the lidar data and so on.

Finally, Fig. 4 depicts the accuracy of temperature profile reconstruction as a function of the level of errors in recording the outgoing radiation and the scheme of interpretation. The plots in Fig. 4 have some peculiarities.

1) All curves originate not from the point (0, 0) but from the points $(0, \Delta\overline{T}_0)$. The value $\Delta\overline{T}_0$ describes the so–called "zero noise" of the algorithm. It is obvious that calculational scheme (5) and quadrature formulas (3) made it possible to essentially decrease the value of $\Delta\overline{T}_0$. It should be noted

that curve *1* in Fig. 4 was obtained, as in Ref. 3, by scheme (4) and using a quadrature formula of trapezoid for unequally spaced nodes during algebraization of Eq. (1).

2) A relatively weak dependence is revealed of $\Delta\overline{T}_0$ on the level of errors in recording the outgoing radiation.

3) Joint processing of data of active (lidar) and passive (IR radiometer) soundings enables one to essentially reduce the "zero noise" of the algorithm for reconstructing $T(\xi)$ and noticeably increase vertical resolution of the passive method of the RTSA what follows from the data presented in Fig. 3.

In conclusion it should be pointed out that the described method for solving the problem of the complex RTSA enables one to make investigations in the field of synchronous ground–based, airborne, and the related experiments and to assimilate *a priori* data on the reconstructed temperature profile obtained by different physical methods into the processing of data of the passive RTSA.

REFERENCES

1. Ph. Russel and M.P. McCormic, Appl. Opt. **21**, No. 9, 1554–1563 (1982).
2. K.Ya. Kondrat'ev and Yu.M. Timofeev, *Thermal Sensing of the Atmosphere from Satellites* (Gidrometeoizdat, Leningrad, 1970), 410 pp.
3. K.Ya. Kondrat'ev and Yu.M. Timofeev, *Meteorological Sounding of the Atmosphere from Outer Space* (Gidrometeoizdat, Leningrad, 1978), 280 pp.
4. I.E. Naats, *Theory of Multifrequency Laser Sounding of the Atmosphere* (Nauka, Novosibirsk, 1980), 157 pp.
5. V.E. Zuev, B.P. Ivanenko, and I.E. Naats, Issled. Zemli iz Kosmosa **5**, 119–121 (1985).
6. O.M. Pokrovskii and Yu. M. Timofeev, Fiz. Atmos. Okeana **7**, No. 1, 12–18 (1971).
7. A. Ya. Tikhonov, *Methods of Solving the Ill–Posed Problems* (Nauka, Novosibirsk, 1979), 282 pp.
8. Yu. M. Timofeev and D. Shpenkukh, in: *Transactions of the International Symposium on Satellite Meteorology* (Gidrometeoizdat, Leningrad, 1977), 21–33 pp.